Solution complexation behaviour of 1,3,5-trioxycyclohexane based ligands and their evaluation as ionophores for Group IA/IIA metal cations

Ofer Reany, Stephanie Blair, Ritu Kataky and David Parker *

Department of Chemistry, University of Durham, South Road, Durham, UK DH1 3LE

Received (in Cambridge, UK) 16th December 1999, Accepted 21st January 2000

A new series of *cis*,*cis*-cyclohexane-1,3,5-triol derivatives bearing one, two and three carbamoylalkyl substituents is reported. Ring interconversion promoted by intramolecular hydrogen bonding is observed for the mono- and di-alkylated derivatives **3** and **4** depending on solvent polarity. ^{1}H NMR parameters obtained have allowed the calculation of the Gibbs free energy change (ΔG^0) for the trioxa-equatorial $\longleftrightarrow$ trioxa-axial equilibrium, modelling the conformational changes promoted by ion binding. Selectivity coefficients have been assessed electrochemically using fixed interference methods for the detection of biologically relevant IA/IIA metal cations. Ionophore **4** displays a Nernstian response towards the detection of Ca^{2+} and $\log K_{Ca,M}^{pot}$ values are calculated. Solution NMR studies confirm the formation of 1 : 1 complexes for **4** with lithium, while 2 : 1 complexation is favoured with Ca^{2+}. Detailed ES-MS studies performed under controlled conditions revealed similar trends in ion binding.

Introduction

Certain polyoxa-polyamide compounds, with low relative molecular mass, have been shown to behave as ionophores or ion carriers.[1] In general, ionophores should display rapid kinetics of complexation and must be highly selective in binding towards the target ion. Ion selective potentiometry is a universal technique that allows the concentration of ions to be monitored for medical and clinical applications. For such analyses, the ionophore should be sufficiently lipophilic to avoid leaching from a polymeric membrane into the aqueous analyte and should be able to transport the target analyte sufficiently quickly that its response is Nernstian over a large range of activities, in the presence of interfering ions.

Over the years, the design of suitable ionophores according to the above guidelines has focused on two main themes, related to the complexation chemistry of the ions involved and the nature and the degree of conformational flexibility of the ligand. Thus, amide carbonyl oxygens are particularly good donors to enhance discrimination in favour of more charge dense cations, *e.g.*, Li^+ and Mg^{2+}. With macrocyclic ionophores (crown-ethers, hemispherands and calixarene derivatives), the smaller ions tend to form more energetically stable complexes when six-membered chelate ring formation occurs, compared to five-membered ring analogues.[2] With acyclic polyamide ionophores, however, these approaches are less straightforward and more detailed investigations of such systems are needed. For example, larger ions such as K^+ and Ca^{2+} prefer to take up higher coordination numbers in their complexes, and the more conformationally flexible acyclic polyamides may competitively form 1 : 2 (ML_2) complexes.

Recently we have investigated a set of oxa-amide ligands based on *cis*,*cis*-cyclohexane-1,3,5-triol[3] (ionophores **6**–**8**, Scheme 1). Good selectivity was observed for Na^+ over K^+ with the C_3-symmetric ligand **8** ($10^{3.1}$), but there was strong interference from Li^+ and Ca^{2+}. Ligands with lower coordination number (*i.e.*, **6** and **7**) gave discrimination in favour of Li^+ (*e.g.* **7**: $10^{2.2}$ for Li^+/Na^+). With this in mind, and as a continuation of a systematic study of *cis*,*cis*-cyclohexane-1,3,5-triol based ligands, we report now the synthesis and ion binding behavior of the related podands **3**–**5**. Successive replacement of each OH group by an oxa-amide allows the ligand denticity to be varied from four to six. The presence of the isobutyl amide groups was proposed to enhance the lipophilicity of the ionophores compared to an *n*-butyl substituent. The nature of the alkyl group in lipophilic amides has been shown to affect both the sensitivity and selectivity of response in ISE measurements.[4] In addition, we have examined the effect of the ligand hydroxy group as a control element in these oxa-amide ionophores (*viz.*, **3** and **4**), determining the conformational flexibility and binding behaviour of the ligands.

Results and discussion

Ionophore synthesis

The oxa-amide ionophores **3**–**5** were prepared from *cis*,*cis*-cyclohexane-1,3,5-triol. Ionophores **4** and **5** were prepared by direct alkylation using the appropriate alkylating agent (*N*,*N*-diisobutyl-2-chloroethaneamide) in the presence of strong base (NaH, DMF, 80 °C, 3 d). Hence, even though one equivalent of alkylating agent was used, only di- and tri-oxa-amide products were obtained accompanied by ether formation *via* a dimerization of the alkylating reagent. Therefore, for the synthesis of the mono oxa-amide ionophore **3**, a rather different reaction sequence was used. Reaction of *cis*,*cis*-cyclohexane-1,3,5-triol with one equivalent of phenylboronic acid, under basic conditions ($NaOH_{aq}$, reflux, overnight), gave a quantitative yield of a stable sodium salt. This product was formulated as **1** on the basis of spectroscopic and analytical data (*cf.* Experimental section) and also by analogy with the structures that have been assigned to the complexes formed from boric acid and *cis*,*cis*-cyclohexane-1,3,5-triol.[5] The sodium salt **1** reacted with *N*,*N*-diisobutyl-2-chloroethaneamide in dimethylformamide to form the corresponding phenylboronate ester **2** in 50% yield. Both steps have the advantage of being monitored by ^{11}B NMR spectroscopy, as neutral boron compounds (*e.g.*, phenylboronic acid and **2**) resonate at *ca.* +30 ppm and the negatively charged boron complex, *e.g.*, **1**, resonates at lower frequency (*ca.* +3 ppm). Compound **2** was treated, with-

DOI: 10.1039/a909906i

Table 1 Selected ^{1}H and ^{13}C NMR data of **3** in (a) $CDCl_3$ and (b) CD_3OD; ((a) 500/125 MHz, (b) 300/75 MHz, δ ppm, J Hz)

	Position	2,6		4				
	Nuclei	eq	ax	eq	ax	1	3,5	OCH_2
(a)	^{1}H	2.11 (dt) ^2J = 12.8 ^3J = 'u'	1.62 (q) ^2J = 12.8 ^3J = 8.4	2.01 (m) ^2J = 'ob' ^3J = 'ob'	1.62 (q) ^2J = 12.8 ^3J = 8.4	3.53 (sept) ^3J = 8.3	3.77 (sept) ^3J = 8.3	4.21 (s)
	^{13}C	38.8		40.8		74.8	65.7	67.6
(b)	^{1}H	2.30 (dt) ^2J = 11.2 ^3J = 'u'	1.17 (q) J = 11.5	2.17 (dt) J = 11.2 ^3J = 'u'	1.20 (q) J = 11.5	3.39 (tt) ^2J = 11.4 ^3J = 3.9	3.53 (tt) ^2J = 11.4 ^3J = 3.9	4.25 (s)
	^{13}C	41.2		45.0		75.2	66.3	68.0

'ob' = peak obscured by the methine (CH) group signal; 'u' = unresolved.

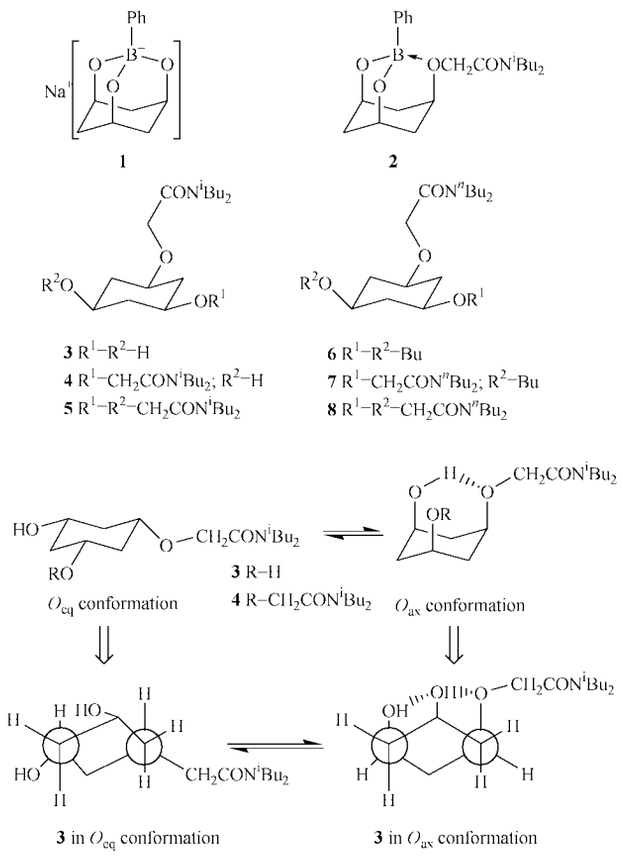

Scheme 1

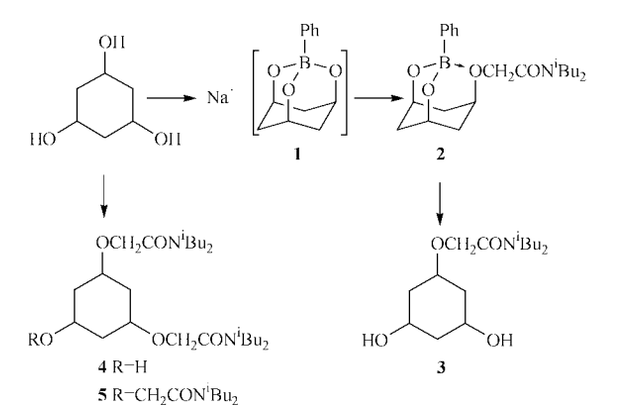

Scheme 2

out further purification, with strong aqueous methanol–sodium hydroxide solution (1 : 1 v/v%), leading to the cleavage of the phenylboronate group and formation of the title compound, **3**, in moderate yield.

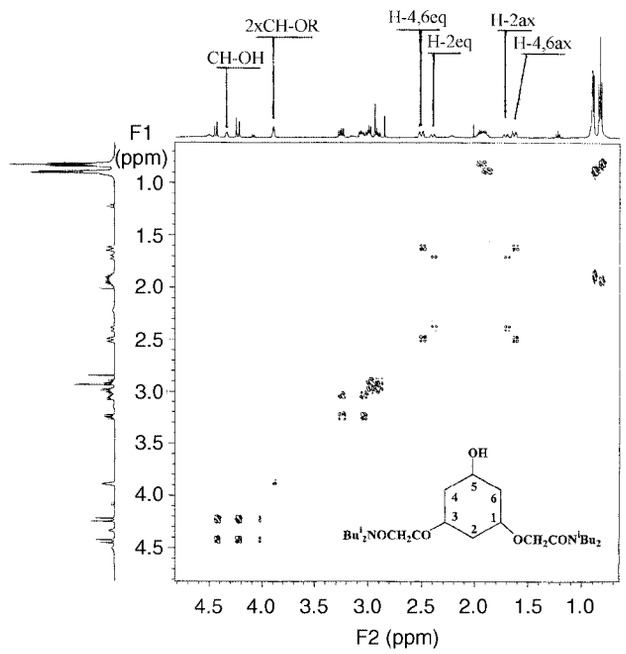

Fig. 1 ^{1}H–^{1}H COSY spectrum of ionophore **4** (295 K; 500 MHz; $CDCl_3$) along with the cyclohexane ring proton assignment.

Conformational analysis of mono oxa-amide 3

^{1}H NMR spectroscopic evidence, primarily based on spin coupling data, confirmed that ionophores **3**, **4** and **5** adopt a chair conformation in solution.[6] A two-dimensional ^{1}H NMR spectrum (COSY) of **4** illustrates the assignment of chemical shifts for mutually coupled protons, *e.g.*, the equatorial and axial protons within a chair conformation (Fig. 1).

The hydroxy and/or oxa-amide groups in **3** and **4** are in *syn*-equatorial or axial sites, depending on the presence of one (or more) intramolecular hydrogen bond interactions (Scheme 1). If two hydroxy groups are positioned in a *syn*-diaxial arrangement, *e.g.* the C^4–C^6 hydroxy groups in glucose and galactose, then a higher conformational energy (*ca.* 4–8 kJ mol^{-1}) is expected compared to the most stable conformer in solution. This unfavorable interaction has been observed in crystal structures of monosaccharides and is referred to as the Hassel-Ottar or 1,3-diaxial effect.[7]

The ^{1}H and ^{13}C NMR spectra of **3** were strongly solvent dependent as exemplified by their behaviour in $CDCl_3$ and CD_3OD. The most noticeable change, in both NMR chemical shifts and coupling constants, was observed for the cyclohexane ring protons.

In $CDCl_3$, the chemical shift difference between equatorial and axial protons H-2,6 and H-4 (termed a Δea value) appeared to be moderately large (Δea = 0.49 and 0.39 ppm respectively) whereas in CD_3OD the Δea values are much bigger, *viz.*, 1.13

Table 2 Relative populations and Gibbs free energy differences for the two possible chair conformations (O_{ax} and O_{eq}) of **3** in solution (295 K, $CDCl_3$)

Entry	[MeOH]/[**3**] molar ratio	H-2,4eq (δ ppm)	H-2,4,6ax (δ ppm)	Δea (ppm)	P_{ax}	K	ΔG^0/kJ mol^{-1}
1	0	2.12	1.62	0.50	0.53	1.11	−0.25
2	1	2.13	1.55	0.59	0.45	0.83	0.46
3	2	2.15	1.49	0.66	0.40	0.65	1.05
4	4	2.16	1.40	0.76	0.31	0.45	2.01
5	6	2.16	1.34	0.82	0.25	0.33	2.72
6	12	2.16	1.27	0.90	0.18	0.22	3.72
7	20	2.15	1.20	0.95	0.11	0.12	5.14
8	30	2.13	1.14	1.00	0.05	0.05	7.19
9	40	2.10	1.09	1.02	<0.05	<0.05	>7.35

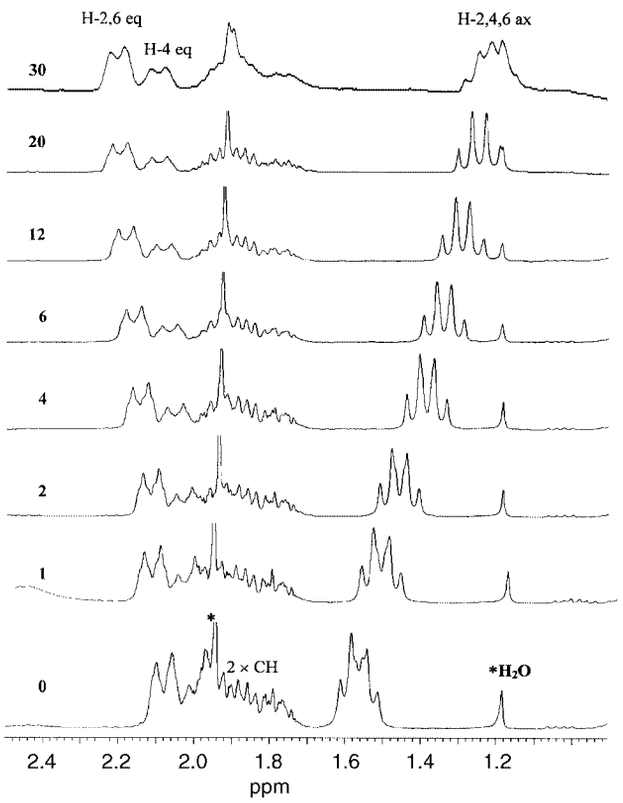

Fig. 2 ^{1}H NMR (300 MHz, $CDCl_3$) spectra recorded in a titration experiment for **3** with incremental addition of methanol. The [MeOH]/[**3**] molar ratios are given on the left of each trace. Asterisk denotes solvent impurities.

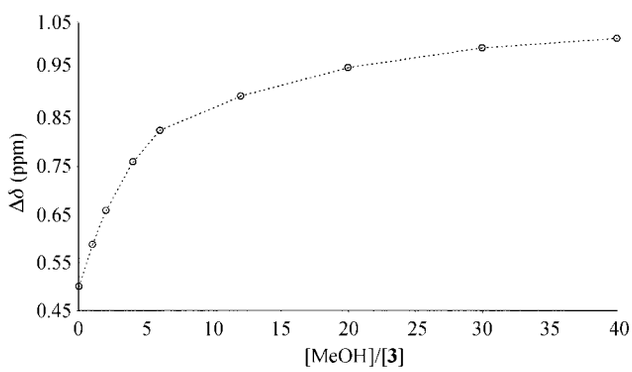

Fig. 3 Plot of chemical shift changes (Δea, see text) *vs.* methanol to ligand molar ratio observed for the ring protons in positions 2, 4 and 6.

and 0.97 ppm respectively. The increase in Δea in methanol is attributed to the deshielding effect of the adjacent electronegative substituents, hydroxy or *O*-alkylated group, suggesting that the predominant conformer is O_{eq}. Similar observations have been reported for the *cis*-cyclohexane-1,3-diol molecule, in which intramolecular hydrogen bonding overcomes the 1,3-diaxial repulsion in aprotic solvents.[8]

Moreover, the ^{1}H NMR spectra of the ring protons display an AB pattern, allowing the dependence of the vicinal coupling constants on the internal HCCH dihedral angle to be defined (Scheme 1). The large vicinal coupling value of 11.4 Hz obtained in methanol-d_4 for $^3J_{H\text{-}1,3,5\text{–}H\text{-}2,4,6ax}$ is consistent with a dihedral angle of 180^0 and again confirms that the predominant conformer in solution is O_{eq}.

Examination of the ^{13}C NMR spectroscopic data for **3** in $CDCl_3$ and CD_3OD solutions reveals that C-2,6 and, in particular, C-4 resonate at considerably higher frequency in the protic solvent. The increased shielding is attributed to the internal *gauche* OCCC moiety in the predominant O_{eq}-conformer, compared to an *anti* arrangement in the O_{ax} form.[9]

In order to quantify the effect of intramolecular hydrogen bonding on the preferred solution conformation of **3**, the free energy difference for the $O_{eq} \longleftrightarrow O_{ax}$ equilibrium was assessed. Thus based on chemical shift differences, the conformational geometry of **3** was perturbed by methanol titration of **3** in $CDCl_3$ solution. The change in the chemical shift differences is illustrated by the spectral sequence for the equatorial and axial H-2,4,6 protons in Fig. 2, with the corresponding titration plot in Fig. 3.

Both conformers of **3** in which the oxa-amide and hydroxy groups are either axial (O_{ax}-conformation) or equatorial (O_{eq}-conformation), Scheme 1, are in rapid equilibrium in solution at room temperature. The mole fraction of the O_{ax}-conformer (P_{ax}) is given directly from the observed chemical shift (δ) as:

$$P_{ax} = (\delta_{obs} - \delta_{ax})/(\delta_{eq} - \delta_{ax}) \quad (1)$$

The free energy difference and equilibrium constant $K = P_{ax}/(1 - P_{ax})$ are thus readily obtained. Comparison between Δea values obtained from solutions in 8.5% methanol in $CDCl_3$ and in CD_3OD (1.01 and 1.13 ppm respectively) revealed that in the presence of 8.5% methanol, 90% of the molecules of **3** exist in the O_{eq} conformation. Thus using the limiting δ_{ax} and δ_{eq} values (Table 2, entry 9) in eqn. (1), the population and Gibbs free energy differences of O_{ax} *vs.* O_{eq} for **3** in $CDCl_3$–MeOH mixtures were assessed.

Similar conformational dynamics have been studied with *cis*-cyclohexane-1,3-diol by NMR[8] and diffusion[10] measurements in different solvents. In both cases, the higher ΔG^0 values obtained in protic solvents implied that hydroxy (or oxa-amide) groups were forming intermolecular hydrogen bonds with the solvent molecules.[10]

These results strongly suggest that the preferred solution conformation is almost entirely determined by the steric effects of the OH and OR groups with 1,3-diaxial interactions favouring the O_{eq} conformation over the O_{ax} conformation in methanol. Consequently, a $\Delta\Delta G$ of more than 7.35 kJ mol^{-1}

provides an estimate of the mean O···O repulsive axial interaction of at least 2.45 kJ mol^{-1}, compared with the estimated $OH_{ax}\cdots OH_{ax}$ repulsive interaction of 3.5 kJ mol^{-1} found in *cis*-cyclohexane-1,3-diol.[8] Further evidence arises from the fact that different signs in ΔG^0 are shown for **3** in $CDCl_3$ (−0.25 kJ mol^{-1}) and 9% methanol in $CDCl_3$ (>7.35 kJ mol^{-1}). Hence in the non-polar solvent, the attractive intramolecular hydrogen bond interactions (more than 3.8 kJ mol^{-1} for each H-bond) are sufficient to overcome the repulsive 1,3-diaxial interactions, thereby promoting ring inversion.

Following the confirmation that intramolecular hydrogen bonding promotes adoption of the O_{ax} conformer, it was anticipated that metal ion binding would impose a similar effect. Cooperative ligation of the ether amide and/or hydroxy oxygens was expected to engender three six-membered ring chelates, in a pseudo-adamantyl array, Scheme 3.

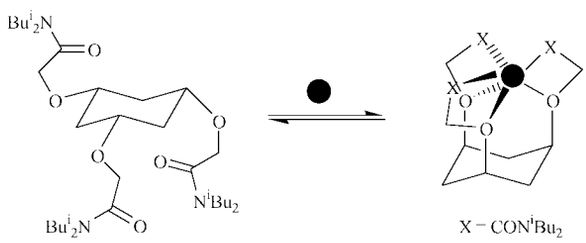

Scheme 3

Electrode response studies

The behaviour of ligands **3**–**5** as ionophores for the detection of selected IA/IIA cations has been compared in standard PVC-based ISE's. Non-Nernstian responses were observed for the mono oxa-amide **3** and trioxa-amide **5** for all the metal ions studied *i.e.*, Li^+, Na^+, K^+, Mg^{2+} and Ca^{2+}. An example of their response towards the detection of Ca^{2+} is shown in Fig. 4 (inset). However an excellent response towards the detection of Ca^{2+} was observed with the diamide ionophore **4**. Comparison with an ISE incorporating the commercially available Ca(II) selective ETH 1001 ionophore revealed similar behaviour, *i.e.*, a Nernstian slope with a limit of detection of $10^{-5.8}$ mol dm^{-3} was found (Fig. 4). Such a response suggests that a 2:1 ionophore–metal ion stoichiometry may be involved, as Ca^{2+} is well known to prefer a co-ordination number of at least six and preferably eight. For the membrane incorporating the relatively polar plasticiser *o*-NPOE, the response was slightly better compared to that for the DOS based membrane, as the high relative permittivity of *o*-NPOE favours divalent cation transport and selectivity.[11] Interestingly, the diamide ionophore **4** shows a quite different pattern of selectivity coefficients for Ca^{2+} as primary ion ($\log K_{Ca,M}^{pot}$), in comparison with the selectivity coefficients found for the di-*n*-butylamide analogue **7** (Table 3). The latter displays marked selectivity over K^+ and Mg^{2+} of $10^{-3.6}$ and $10^{-4.2}$, but poorer selectivity over Na^+ and Li^+ ($10^{-0.6}$ and $10^{0.9}$ respectively). In contrast, ionophore **4** displays enhanced selectivity over Na^+ and Li^+ of $10^{-2.3}$ and $10^{-1.9}$, but lower selectivity over K^+ and Mg^{2+} of $10^{-2.2}$ and $10^{-2.7}$ respectively.

Using an ISE incorporating the ionophore **4**, the response for Ca^{2+} was measured in the presence of a simulated extracellular background of interfering ions (140 mM NaCl, 4.3 mM KCl, 0.9 mM $MgCl_2$). Given that the free extracellular Ca^{2+} concentration range is typically between 1.16 and 1.32 mM, the electrode was able to measure the Ca^{2+} concentration with a Nernstian response in this region (Fig. 5). The sub-Nernstian response of the triamide ionophore **5** suggested that this ionophore may bind to Ca^{2+} too strongly. Slow decomplexation kinetics may prevent rapid transport from occurring at the interfacial region of the membrane. Such behaviour is consistent with the reported stabilities of the *n*-butylamide Ca^{2+} complexes.[3] A significant difference in binding strength of the dioxa-amide **7** ($10^{3.6}$) compared with the trioxa-amide **8** ($10^{>5.5}$) was revealed by ^{13}C NMR titration data (*vide infra*).

Table 3 Selectivity coefficients for calcium ISE's based on the diamide ionophores **4** and **7** (298 K)

	Selectivity $\log K_{Ca,M}^{pot}$			
Ionophore	Na^+	K^+	Mg^{2+}	Li^+
4	−2.3	−2.2	−2.7	−1.9
7	−0.6	−3.6	−4.2	0.9

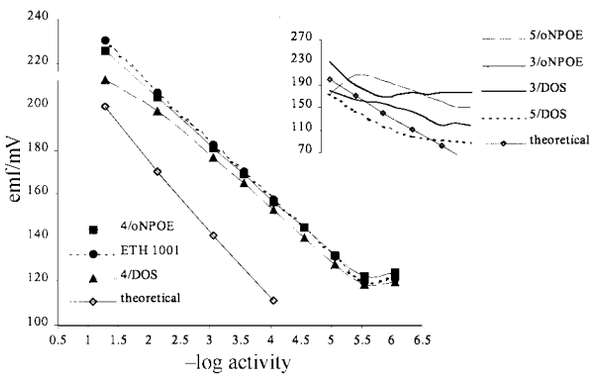

Fig. 4 Response curves for Ca^{2+} obtained with an electrode based on **4** using different plasticizers (see text), in comparison to theoretical and commercially available ETH 1001 electrode. The inset shows the response for electrodes based on **3** or **5** towards Ca^{2+} (298 K). [*o*-NPOE is *o*-nitrophenyl octyl ether and DOS is bis(2-ethylhexyl) sebacate; ETH 1001 is (−)-(*R*,*R*)-*N*,*N*′-bis[11-(ethoxycarbonyl)undecyl]-*N*,*N*′-4,5-tetramethyl-3,6-dioxaoctanediamide].[11,24,25]

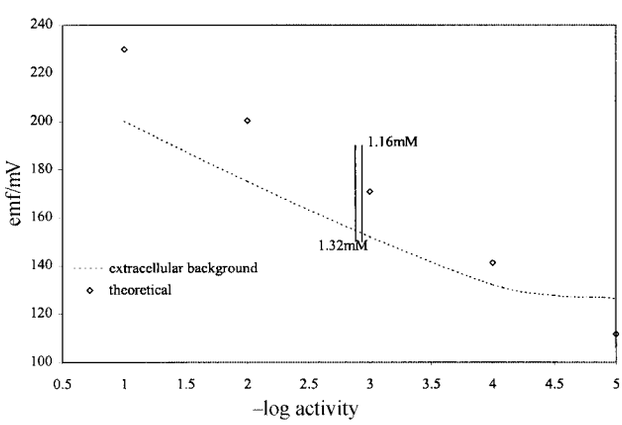

Fig. 5 Response curve for Ca^{2+} obtained with the electrode based on **4** in the presence of interfering ions, of concentrations similar to those found in extracellular fluids (298 K; 140 mmol dm^{-3} Na^+, 4.3 mmol dm^{-3} K^+, 0.9 mmol dm^{-3} Mg^{2+}).

Spectroscopic investigation of solution complexation

Following the results obtained from the electrode response studies, further proton NMR studies (400 MHz, CD_3OD) were undertaken to gain more information about the complexation behaviour of ionophores **4** and **5** in solution. Incremental addition of lithium perchlorate in methanol-d_4 solution of **4** (22 mmol) resulted in significant spectral changes. The most noticeable shifts were observed for the ring protons and the OCH_2 units; the metal ion presumably promoted ring interconversion through a relatively strong cooperative interaction with the ether and amide oxygens. Nevertheless, it should be borne in mind that methanol is a strongly competitive ligand for the free Li^+ ion, and the relative ease of lithium exchange

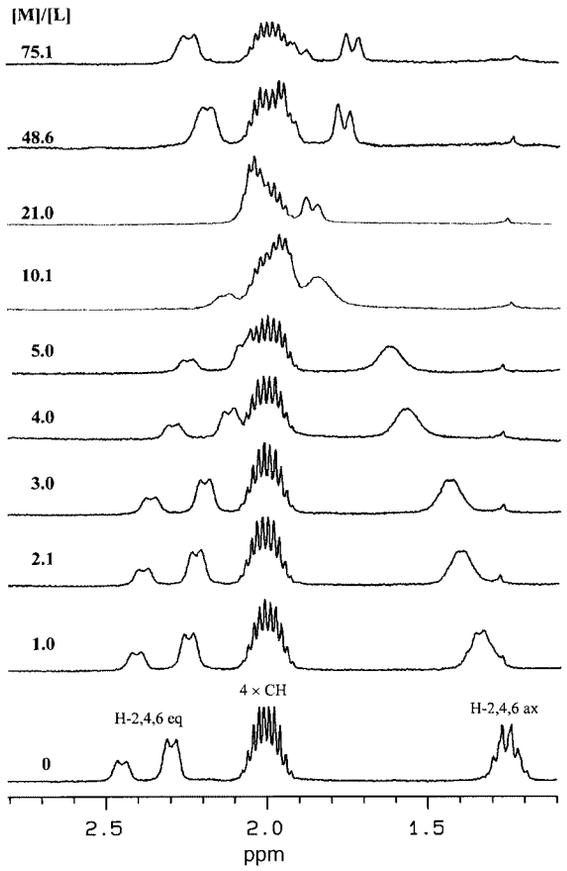

Fig. 6 Selected ^{1}H NMR spectroscopic data (400 MHz, CD_3OD) for titration of ionophore **4** following incremental addition of $LiClO_4$. The [Li]/[**4**] molar ratios are shown on the left.

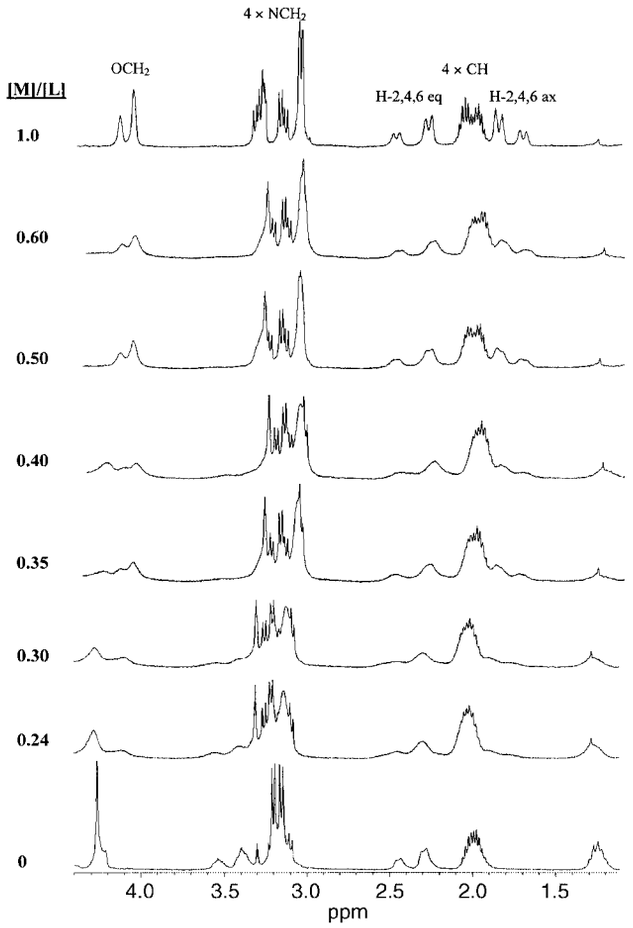

Fig. 7 Selected ^{1}H NMR spectroscopic data (400 MHz, CD_3OD) for titration of ionophore **4** with incremental addition of $Ca(NO_3)_2$ tetrahydrate. The [Ca]/[**4**] molar ratios are indicated on the left.

(*i.e.*, between solvated and bound states) was indicated by the form of the titration curve. Only in the presence of a large excess of Li^+ ion (*ca.* ×75) was the limiting spectrum reached (Fig. 6).

Attempts were made to fit the titration curve by a model involving simply 1 : 1 complex formation using an iterative least-squares analysis. However, the calculated values fitted to the experimental points showed a noticeable deviation in the titration curve at high salt to ionophore ratios. This is most likely to be associated with the increasing ionic strength of the solution as the concentration of lithium salt in the solution exceeded 1.65 M. We then used a graphical approach, *i.e.*, the NMR equation analogue of the well known Benesi–Hildebrand binding isotherm:[12]

$$\Delta^{-1} = (K_c\Delta^0[\mathrm{Li}])^{-1} + (\Delta^\circ)^{-1} \quad (2)$$

$\Delta = \delta_{obs} - \delta_L$ and $\Delta^0 = \delta_{ML} - \delta_L$; δ is the chemical shift of a specific NMR signal for 'free' (δ_L) and 'bound' (δ_{ML}) ligand and (δ_{obs}) the observed chemical shift under conditions of fast exchange rate on the NMR timescale. A major limitation of eqn. (2) relates to the linear double reciprocal plot: Δ^0 is evaluated from a relatively small intercept and may be subject to an error which is reflected in K_c, especially for weak complexes.[13] Of the many alternative transformations suggested for eqn. (2), a method was chosen[14] involving the independent determination of the binding constant K_c and the chemical shift of the pure complex in the expression of Δ^0. Hence, a simple rearrangement of eqn. (2) gives either eqn. (3) or (4):

$$[\mathrm{Li}]_t = \Delta^0[\mathrm{Li}]_t/\Delta - K_c^{-1} \quad (3)$$

$$\Delta = \Delta^0 - \Delta K_c^{-1}[\mathrm{Li}]_t^{-1} \quad (4)$$

In both forms, K_c and Δ^0 are calculated separately and can be determined from the slope of each equation. Linear fitting of the plots obtained from eqns. (3) and (4) using chemical shift data for H-2,4,6 gave an estimated $\mathrm{Log}K_{1:1}$ value of 0.60 ± 0.05 and limiting Δ^0 value of 1.15 ± 0.03 ppm.

A similar titration of ionophore **4** with $Ca(NO_3)_2$ was undertaken. Incremental addition of the salt gave, this time, separate ^{1}H NMR signals for the 'free' and 'bound' ligand protons up to a stoichiometry of 1 : 2 metal to ligand ratio (*viz.*, ML_2 formation). Thereafter only resonances due to the complexed ionophore were observed (Fig. 7). At higher Ca^{2+} concentrations the signals were slightly sharper than in the spectrum obtained for a [M]/[L] ratio of 0.54. Such behaviour is consistent with the formation of a relatively stable 1 : 2 complex (ML_2) with $4.5 \leq \log K \leq 5.5$, as the exchange between 'free' and 'bound' complex is slow on the NMR timescale, but some line broadening was observed (298 K, 400 MHz).

Electrospray (ES) mass spectroscopic studies

Electrospray ionisation mass spectrometry (ESI-MS) has proved to be a valuable tool in studying the binding of metal ions to synthetic ionophores.[3,15–17] However, it is important to use ESI-MS to determine solution speciation with circumspection and to ensure that suitable control experiments are performed.

Although the detailed mechanism of ion production in ESI-MS remains obscure[18] there are some established features which suggest how the complex ions produced arise from the solution. In positive ESI-MS the sample solution emerges into the source *via* a needle held at a positive potential relative to a

collector plate in the low-pressure region. Consequently, anions in the solution will migrate towards the needle, while cations will be repelled into the droplets that spray into the source, and eventually, produce the cations observed in the mass spectrometer detector *via* a process of solvent evaporation and droplet fission.

The two proposed mechanisms of ESI, the single ion droplet theory by Dole[19] and the ion evaporation model by Iribarne and Thomson[20] both imply that the nature of the ions in solution affects their desolvation and release from droplets into the gas phase. Therefore surface activity and relative evaporation rates of ions are dominant factors that influence the response factors in ESI. Optimal experimental conditions (cone voltage, ligand/ion concentrations) have been developed recently[3] which may prevent distortion of the species distribution from occurring especially during ion transfer through the ES interface and in the mass analyser and detector.

The oxa-amide ionophores **6**–**8** (Scheme 1) showed selective metal ion complexation according to ISE measurements, and detailed ESI-MS studies confirmed the order of selectivity in ion binding, under controlled conditions.[3] The order of selectivity for ionophores **4** and **5** has been examined by two different approaches. In experiments where only the metal ion of interest is present in excess, the intensity of signal which appeared for the 'bound' ionophore $[ML]^{n+}$ with the ion of interest was compared to uncomplexed ligand (as the protonated form $[M\mathrm{H}]^+$) or 'bound' with Na^+ $[M\mathrm{Na}]^+$ species. In experiments where more than one metal was present in solution, the relative intensities measured for different metal complexes (*e.g.*, $M\mathrm{Li}^+$, $M\mathrm{Na}^+$, $M\mathrm{K}^+$ *etc.*) were used to determine a selectivity order. Obviously in such experiments desolvation energy plays an important role in the determination of the ES-MS response factor. Different metal ions and metal complexes (as their structure possibly includes solvent molecules or a different stoichiometry) require different desolvation energies, and consequently may perturb the analysis of the species distribution in solution.

Solutions containing the host and a single guest cation were prepared at a concentration ratio of 1:10. In a second set of experiments, solutions containing the host and two or more competing ions were prepared at a concentration ratio of 1:10:10:*etc.*† No protonated adducts were observed while assessing the alkali metal complexes of **4**, indicating that metal complexation was favourable under the electrospray conditions. The determined selectivity parameters, in Table 4, show agreement with the expected trend in ion selectivity, as deduced from the electrode response studies *i.e.*, binding selectivity of ionophore **4** follows the order of Li > Na > K.

Competition experiments were then carried out, for each singly charged cation, allowing equimolar concentrations of the metal ions to compete for a deficiency of the ligand, a procedure that has been used previously.[3,21] Selectivity ratios for I_{Na^+}/I_{Li^+} and I_{Na^+}/I_{K^+} of 0.11 (0.03) and 1.4 (0.3) were assessed, reflecting the expected trend from the ISE studies.

One explanation for the quantitative dissimilarity in the selectivity data could relate to the fact that in the mixed metal ions solution, the larger cation with low charge density is more likely to desolvate and hence preferentially tends to migrate to the surface of the droplet to minimise charge-repulsion. Already at this stage, the 'solution phase' of the parent droplet is far from a well-mixed homogeneous equilibrium. Consequently, there is a better chance for the less desolvated metal ion (*e.g.*, Li^+) in the centre of the parent droplet to interact with the 'free' ligand. The increased selectivity ratios for I_{Na^+}/I_{Li^+} and I_{Li^+}/I_{K^+} support such a heterogeneous equilibrium. Moreover, assuming that potassium enrichment at the droplet surface occurs in such a heterogeneous equilibria ion binding is a means to reduce electrostatic repulsion between adjacent metal cations and a reduced selectivity ratio for I_{Na^+}/I_{K^+} is observed.

Table 4 ES-MS determined selectivity parameters for ligand **4** (110 V cone voltage, 4 kV capillary voltage, **4** = 1×10^{-5} mol dm^{-3}, 20 μdm^{-3} injection loop)

M^+	I_{Na^+} [a]	I_{M^+}	I_{Na^+}/I_{M^+} [b]
Li^+	2.9 (0.2)	16.6 (0.7)	0.18 (0.02)
K^+	13.6 (1.1)	2.4 (0.5)	5.8 (0.8)

[a] Each figure given is the mean for three sets of experiments for each of which the given peak intensity represents the mean of *ca.* 500 scans in the plateau region of the ion-current. [b] Error reported was the standard deviation of all spectra recorded.

Similar sets of experiments were performed with ligand **4** using alkaline earth metal ions. Different cone voltage potentials caused diverse patterns or changes in relative peak intensities. Associated anion adducts of the alkaline earth metals were observed. The relative intensities obtained from the mixed metal complexation experiment were examined. Fortunately, it was possible to eliminate most of the addition peaks assigned to solvent and anion adducts by using a 20 V cone voltage. Hence, four molecular ion masses were indicated: $[M\mathrm{Sr}]^{2+}$ (279 *m*/*z*, 15%), $[M\mathrm{Ca(MeOH)}]^{2+}$ (271 *m*/*z*, 80%), $[M\mathrm{Ca}]^{2+}$ (255 *m*/*z*, 100%) and $[M\mathrm{Mg}]^{2+}$ (247 *m*/*z*, 30%), where *M* = [**4**]. Although there are two peaks related to Ca(II) complexes one cannot ignore the distinct selectivity order trend found here, *i.e.*, $Ca^{2+} \gg Mg^{2+} > Sr^{2+}$, in harmony with the results of the ISE measurements.

For the ionophore **5**, the ISE and NMR studies had demonstrated that Ca^{2+} formed a particularly strong complex. A single peak for $[M\mathrm{Ca}]^{2+}$ was even seen for the 'free' ionophore. Using a ten fold excess of various metal ions, *viz.*, Li^+, Na^+, K^+, Mg^{2+} and Sr^{2+} as an interferent ion background, the peak due to the calcium complex remained strong and no additional peaks were observed, other than a second peak assigned to $[M\mathrm{Ca(anion)}]^+$ with a higher intensity than the original $[M\mathrm{Ca}]^{2+}$ signal. The anion adducts varied according to the metal salt that had been used.

Conclusion

A series of oxa-amide ionophore derivatives based on *cis*,*cis*-cyclohexane-1,3,5-triol has been prepared with ligand co-ordination numbers of four (compound **3**), five (**4**) and six (**5**). The ring interconversion equilibrium of **3** is a function of the nature of the solvent: ligand **3** takes up a conformation with triaxial C–O bonds in chloroform due to an intramolecular hydrogen bonding effect.

Solution complexation studies highlight the selectivity of ionophore **4** for Ca^{2+}. The formation of 2:1 ionophore metal–ion stoichiometry is shown for **4** towards Ca^{2+}. ES-MS studies on **4**, under controlled conditions, have shown a reliable qualitative order of complexing ability; a similar trend in ion binding behaviour for ionophore **5** was observed, with a high selectivity for Ca^{2+}. Given that a typical extracellular ionized Ca^{2+} concentration range[26] is 1.16–1.32 mmol dm^{-3}, the electrode incorporating ionophore **4**, in the presence of a simulated extracellular background of interfering ions, is able to measure the calcium concentration with a Nernstian response in this region.

† Signal intensities *versus* analyte concentration began to deviate from linearity at concentrations below 10^{-5} mol dm^{-3} because of the lower limit of signal detection that can be reached. Detection of lower concentrations is possible if the instrumental parameters were adjusted (*e.g.*, ESI source temperature, flow rate *etc.*) but the experimental parameters (except concentration) were kept constant within the data set.

Experimental

Electrospray mass spectrometry

Spectra were recorded with a VG Platform II (Fisons Instruments) employing Mass Lynx software. Samples were presented as solutions in methanol (Aristar Grade, BDH) at a flow rate of 0.01 $cm^3\ min^{-1}$.

Solutions were made up in glassware flasks. Samples were prepared using Gilson Pipetman micropipettes in polypropylene Eppendorf tubes. Glassware was washed with hot nitric acid, thoroughly rinsed with de-ionised water and dried. The spectrometer was operated in positive ion mode, with a capillary voltage of 4 kV and a source temperature of 60 °C. Mass scale calibration employed NaI. HPLC grade methanol (Fisons) was used as a background (carrier) solvent into which the samples were 'injected'. Cone voltages were varied according to the nature of the experiment (see text) and ranged from 20 to 140 V.

The solvent flow was maintained using a Hewlett-Packard HPLC instrument that was directly linked to the ES mass spectrometer. The sample was inserted into the flow using an injection valve with a 20 μl steel loop and transported to the electrospray capillary through a silica tube. The injection valve and tubing were flushed through with a variety of solvents from dichloromethane to de-ionised water prior to experiments being performed.

Potentiometric studies

The membranes were prepared by dissolving 1.3% w/w ionophore, 65.6% w/w *o*-nitrophenyl octyl ether (*o*-NPOE) or bis(2-ethylhexyl) sebacate (DOS) plasticiser (Fluka), 32.8% w/w PVC (high molecular mass, Fluka) and 0.5% w/w potassium tetrakis(4-chlorophenyl)borate (Fluka) in 1.5 ml distilled tetrahydrofuran. Membranes of ~200 μm thickness were obtained by casting the solution into a glass ring (37 mm internal diameter), fixed on a glass plate. Discs, 7 mm in diameter, were cut from the master membranes and mounted in standard electrode bodies supplied by Fluka. The inner electrolyte was a 10^{-3} mol dm^{-3} solution of the relevant metal chloride salt. The electrodes were immersed over 24 h in a 10^{-2} mol dm^{-3} solution of the metal chloride salt for preconditioning prior to use.

Electrode calibration was performed at 298 K according to the Separate Solution Method (SSM).[22] Calibration solutions of the metal chloride salt were prepared at decade intervals of concentration in the range of 10^{-1} to 10^{-3} mol dm^{-3}, and half decade intervals of concentration in the range of 10^{-3} to 10^{-6} mol dm^{-3}. EMF measurements were recorded on a Molspin Ltd 4 input voltmeter.

Selectivity coefficients K_{ij}^{pot}, where i is the primary ion and j is the interfering ion, were determined at 298 K according to the Fixed Interference Method (FIM: $j = 0.1$ M), using the technique of constant volume dilution.[23] A buffer amplifier interfaced to a Thurlby Thandler 1705 multimeter and a chart recorder (Kipp and Zenen) recorded measurements.

All measurements were made against a double junction type Ag/AgCl external reference electrode.

Syntheses

All reactions were carried out in apparatus which had been oven-dried and cooled under argon. All solvents were dried by distillation from an appropriate drying agent and water was purified from the 'Purite' system. Silica refers to Merck silica gel F60 (230–400 mesh).

Varian Mercury-200 and Varian Unity-300 NMR operating at 199.9 and 299.9 MHz for ^{1}H NMR, and 96.2 MHz *for* ^{11}B NMR, were used routinely to identify and monitor reaction products. Spectra were determined with a Varian Inova-500 operating at 499.8 and 125.7 MHz for ^{1}H (COSY) and ^{13}C (C–H correlation, DEPT) NMR respectively. All chemical shifts are given in ppm relative to the residual solvent resonance and coupling constants (J) are in Hz. The titration experiments were carried out using a Varian VXR-400 NMR operating at 399.9 MHz for ^{1}H NMR.

For the ^{1}H NMR titration studies, a known mass—*ca.* 12–16 mg—of the ligand (*e.g.*, **4**, **5**) was dissolved in methanol-d_4 (*ca.* 1.5 cm^3) to give a total 0.022–5 mM concentration. Amounts of anhydrous lithium perchlorate or calcium nitrate dihydrate were weighed and dissolved in methanol-d_4 (*ca.* 0.75 cm^3) to give 1 M stock solutions. The salts were added sequentially by Gilson Pipetman micropipettes in polypropylene Eppendorf tubes (*ca.* 1 μL) and the NMR spectrum was recorded. A plot of the variation of the change in chemical shift for selected ligand resonances was made as a function of the added salt (see text).

***cis*,*cis*-Phenyl(cyclohexane-1,3,5-triyltrioxy)borate sodium salt, 1.** To an aqueous solution (15 mL) of *cis*,*cis*-cyclohexane-1,3,5-triol dihydrate (3 g, 19.0 mmol) sodium hydroxide (0.93 g, 0.023 mol) was added at room temperature. The reaction mixture was heated to about 70 °C and phenylboronic acid (2.6 g, 21 mmol) was added in one portion. The mixture was maintained at 70–80 °C. Five hours were needed to complete reaction, as monitored by proton and/or boron NMR. The solution was allowed to cool to room temperature, the solvent was removed under reduced pressure to yield a white powder salt, in quantitative conversion. The title compound was used without further purification immediately thereafter. ^{1}H NMR (300 MHz, $CDCl_3$) 1.69 (br d, $J = 12.5$ Hz, 3H, H-2,4,6_{ax}), 2.23 (br d, $J = 12.5$ Hz, 3H, H-2,4,6_{eq}), 4.12 (br s, 3H, H-1,3,5_{eq}), 7.15 (m, $3H_{aryl}$), 7.33 (m, $2H_{aryl}$); ^{11}B NMR (96.2 MHz, D_2O) 3.82 (br s).

***cis*,*cis*-1,3-(Phenylboranediyldioxy)-5-(*N*,*N*-diisobutylcarbamoylmethoxy)cyclohexane, 2.** The crude salt of **1** was dissolved in dimethylformamide (50 ml) containing molecular sieves and 4-*N*,*N*-diisobutylbromoacetamide (5.3 g, 21 mmol) was added in one portion. The reaction mixture was heated at 60–70 °C under argon, until ^{11}B NMR-control showed the consumption of **1**. At that time, the reaction mixture was allowed to cool and the insoluble material filtered off. The remaining filtrate was diluted with water and then extracted with diethyl ether employing a continuous extraction technique. The ethereal solution was then dried ($CaCl_2$), filtered and concentrated to dryness to yield pale yellow oil of **2**, which was immediately reacted in the next step. ^{11}B NMR (96.2 MHz, $CDCl_3$) 29.5 (br s).

***cis*,*cis*-1,3-Dihydroxy-5-(*N*,*N*-diisobutylcarbamoylmethoxy)-cyclohexane, 3.** The intermediate compound **2** was dissolved in 0.5 M sodium hydroxide in an aqueous–methanol mixture (1 : 1 v/v). The solution was heated at reflux under argon for 6 h. Methanol was removed under reduced pressure and the concentrated aqueous solution was extracted with dichloromethane employing continuous extraction. The organic solution was then dried ($CaCl_2$), filtered and the solvent removed under reduced pressure. The crude product was purified by column chromatography (silica gel, ethyl acetate) eluting with ethyl acetate–methanol–ammonia [80 : 19 : 1], to yield an off-white semi-solid, which upon standing gave colourless crystals (1.89 g, 33% from **1**). Mp 51–53 °C. Found (ES-MS) 324.2148; $C_{16}H_{31}NO_4 + Na^+$ requires 324.2151. ^{1}H NMR (500 MHz, $CDCl_3$) 0.85 (d, $J = 6.5$ Hz, 6H, 2 × Me), 0.89 (d, $J = 6.5$ Hz, 6H, 2 × Me), 1.62 (m, 3H, H-2,4,6_{ax}), 1.92 (septet, $J = 6.5$ Hz, 1H, CH), 2.0 (m, 2H, CH + H-4_{eq}), 2.10 and 2.12 (2 × br t, 2H, H-2,6_{eq}), 3.03 (d, $J = 7.5$ Hz, 2H, NCH_2), 3.16 (d, $J = 7.5$ Hz, 2H, NCH_2), 3.53 (m, 1H, H-1_{eq}), 3.77 (m, 2H, H-3,5_{eq}); ^{13}C NMR (125.7 MHz, $CDCl_3$) 20.0 and 20.1 (2 × Me), 26.2 and 27.3 (2 × CH), 38.8 (C-2,6), 42.0 (C-4), 52.7 and 54.1

(2 × NCH_2), 65.7 (C-3,5), 67.6 (OCH_2CO), 74.8 (C-1); MS (*ES*$^+$) *m*/*z* 324 (*MNa*$^+$), 625 (*M*$_2$*Na*$^+$).

***cis*,*cis*-1,3-Bis(*N*,*N*-diisobutylcarbamoylmethoxy)-5-hydroxycyclohexane, 4 and *cis*,*cis*-1,3,5-tris(*N*,*N*-diisobutylcarbamoylmethoxy)cyclohexane, 5.** Anhydrous *cis*,*cis*-cyclohexane-1,3,5-triol (1.11 g, 6.6 mmol) was dissolved in dry dimethylformamide (10 ml) under argon. Sodium iodide (0.99 g, 6.6 mmol), sodium hydride (0.16 g, 6.6 mmol), and *N*,*N*-diisobutylbromoacetamide (1.65 g, 6.6 mmol) were added and the solution mixture was heated at 80 °C under argon. After 5 d the excess of sodium hydride was quenched with 1 ml of water, the suspension filtered and solvent was removed *in vacuo* (100 °C, 0.1 mmHg). The residue was purified by column chromatography on silica gel. Ionophore **4** (0.42 g, 0.895 mmol) was obtained as pale yellow oil, following elution with ethyl acetate–methanol–NH_3 [89 : 9 : 1], in 14% yield; ionophore **5** (0.106 g, 0.165 mmol) was eluted later with ethyl acetate–methanol–NH_3 [84 : 15 : 1] and was obtained as pale yellow oil in 3% yield.

4: Found (ES-MS) 493.3613; $C_{26}H_{50}N_2O_5$+Na^+ requires 493.3617. ^{1}H NMR (500 MHz, $CDCl_3$) 0.82 (d, *J* = 7.8 Hz, 12H, 4 × Me), 0.89 (d, *J* = 7.8 Hz, 12H, 4 × Me), 1.62 (dt, *J* = 15.5, 3.5 Hz, 2H, H-4,6$_{ax}$), 1.69 (dt, *J* = 15.5, 3.5 Hz, H, H-2$_{ax}$), 1.92 (m, 2H, 2 × CH), 2.39 (br d, *J* = 15.5 Hz, 1H, H-2$_{eq}$), 2.39 (br d, *J* = 15.5 Hz, 2H, H-4,6$_{eq}$), 2.89 (dd, *J* = 15, 8 Hz, 1H, NCH_2), 2.99 (dd, *J* = 15, 7.2 Hz, 1H, NCH_2), 3.05 (dd, *J* = 13.5, 7.5 Hz, 1H, NCH_2), 3.24 (dd, *J* = 13.5, 7.5 Hz, 1H, NCH_2), 3.88 (br s, 2H, H-1,3$_{eq}$), 4.22 (d, *J* = 14 Hz, 2H, OCH_2), 4.33 (br s, 1H, H-5$_{eq}$), 4.42 (d, *J* = 14 Hz, 2H, OCH_2), 4.50 (br s, 1H, OH); ^{13}C NMR (125.7 MHz, $CDCl_3$) 20.0, 20.1, 20.2 and 20.3 (4 × Me), 26.2 and 27.4 (2 × CH), 32.0 (C-2), 33.0 (C-4,6), 53.0 (2 × NCH_2), 54.2 (2 × NCH_2), 32.1 (C-1), 67.7 (2 × OCH_2CO), 72.6 (C-3,5); MS (*ES*$^+$) *m*/*z* 493 (*MNa*$^+$), 735 (*M*$_2$*Na*$^+$).

5: Found (ES-MS) 339.7410; $C_{36}H_{69}N_3O_6$+Ca^{2+} requires 339.7406. ^{1}H NMR (500 MHz, $CDCl_3$) 0.89 (d, *J* = 7.5 Hz, 24H, 8 × Me), 0.95 (d, *J* = 7.5 Hz, 12H, 4 × Me), 1.98 (m, 9H, 3 × CH + H-2,4,6$_{ax}$), 2.68 (br d, *J* = 15.5 Hz, 3H, H-2,4,6$_{eq}$), 3.01 (d, *J* = 7.5 Hz, 6H, 3 × NCH_2), 3.19 (d, *J* = 7.5 Hz, 6H, 3 × NCH_2), 4.29 (br s, 3H, H-1,3,5$_{eq}$), 4.71 (s, 6H, 3 × OCH_2); ^{13}C NMR (125.7 MHz, $CDCl_3$) 20.2 and 20.4 (12 × Me), 26.3 and 27.3 (6 × CH), 31.6 (C-2,4,6), 53.6 and 54.6 (6 × NCH_2), 70.9 (3 × OCH_2CO), 74.2 (C-1,3,5); MS (*ES*$^+$) *m*/*z* 340 (*MCa*$^{2+}$) 741 (*MCaNO*$_3^+$).

Acknowledgements

We thank EPSRC and BBSRC for support, the Royal Society for a Leverhulme Trust Senior Research Fellowship (D. P.), the EPSRC National MS service (Swansea) for accurate mass determinations, and Dr Ray Houghton (Swansea) for stimulating discussions.

References

1 Many examples of amide type ionophores are cited in recent reviews on carrier-based ISE's: E. Bakker, P. Buhlmann and E. Pretsch, *Chem. Rev.*, 1997, **97**, 3083; P. Buhlmann, E. Pretsch and E. Bakker, *ibid.*, 1998, **98**, 1593.
2 R. D. Hancock, *Pure Appl. Chem.*, 1986, **58**, 1445.
3 M. Goodall, P. M. Kelly, D. Parker, K. Gloe and H. Stephan, *J. Chem. Soc.*, *Perkin Trans. 2*, 1997, 57.
4 E. Metzger, D. Ammann, R. Asper and W. Simon, *Anal. Chem.*, 1986, **58**, 132; V. P. Y. Gadzekpo, J. M. Hungerford, A. M. Kadry, Y. M. Ibrahim, R. Y. Xie and G. D. Christian, *ibid.*, 1986, **58**, 1948.
5 S. J. Angyal and D. J. McHugh, *J. Chem. Soc.*, 1957, 1423; J. Dale, *J. Chem. Soc.*, 1961, 922; J. Dale, *J. Chem. Soc.*, 1965, 389.
6 E. L. Eliel, N. L. Allinger, S. J. Angyal and G. A. Morisson, Eds., in *Conformational Analysis*, Wiley-Interscience, 1965, p. 152.
7 G. A. Jeffrey and W. Saenger, *Hydrogen Bonding in Biological Structures*, Springer-Verlag, Berlin, 1991, p. 184.
8 R. J. Abraham, E. J. Chambers and W. A. Thomas, *J. Chem. Soc.*, *Perkin Trans. 2*, 1993, 1061.
9 E. Breitmaier and W. Voelter, *Carbon-13 NMR Spectroscopy—High Resolution Methods and Applications in Organic Chemistry and Biochemistry*, 3rd Edn., VCH Weinheim, 1990.
10 T. Tominaga, S. Tenma and H. Watanabe, *J. Chem. Soc.*, *Faraday Trans.*, 1996, **92**, 1863.
11 P. Anker, E. Wieland, D. Ammann, R. E. Dohner, R. Asper and W. Simon, *Anal. Chem.*, 1981, **53**, 1970; D. Ammann, R. Bissig, M. Guggi, E. Pretsch, W. Simon, I. J. Borowitz and L. Weiss, *Helv. Chim. Acta*, 1975, **58**, 1535; W. E. Morf and W. Simon, *Helv. Chim. Acta*, 1971, **54**, 2683.
12 H. Benesi and J. H. Hildebrand, *J. Am. Chem. Soc.*, 1949, **71**, 2703.
13 K. A. Connors, '*Binding Constants, The Measurement of Molecular Complex Stability*', Interscience, 1987.
14 B. K. Seal, A. K. Mukherjee, D. C. Mukherjee, P. G. Farrell and J. V. Westwood, *J. Magn. Reson.*, 1983, **51**, 318.
15 J. B. Fenn, M. Mann, C. K. Meng, S. W. Wong and C. M. Whitehouse, *Science*, 1989, **246**, 64.
16 E. Leize, A. Van Dorsselaer, R. Kramer and J.-M. Lehn, *J. Chem. Soc.*, *Chem. Commun.*, 1993, 990; G. Hopfgartner, C. Piquet, J. D. Henion and A. F. Williams, *Helv. Chim. Acta*, 1993, **76**, 1759; P. S. Bates, B. N. Green and D. Parker, *J. Chem. Soc.*, *Chem. Commun.*, 1993, 650; E. Leize, A. Jaffrezic and A. Van Dorsselaer, *J. Mass Spectrom.*, 1996, **31**, 537.
17 T. M. Fyles and B. Zeng, *Supramol. Chem.*, 1998, **10**, 143; W. Z. Shou and R. F. Browner, *Anal. Chem.*, 1999, **71**, 3365; K. Kimura, R. Mizutani, M. Yokoyama and R. Arakawa, *Anal. Chem.*, 1999, **71**, 2922; A. Tsuda, H. Moriwaki and T. Oshima, *J. Chem. Soc.*, *Perkin Trans. 2*, 1999, 1235.
18 G. Agnes and G. Horlick, *Appl. Spectrom.*, 1992, **46**, 401; *ibid.*, 1994, **48**, 649 and 655; *ibid.*, 1995, **49**, 324.
19 M. Dole, L. L. Mack, R. L. Hines, R. C. Mobley, L. D. Ferguson and M. B. Alice, *J. Chem. Phys.*, 1979, **71**, 4451.
20 J. V. Iribarne and B. A. Thomson, *J. Chem. Phys.*, 1976, **64**, 2287.
21 S. M. Blair, E. C. Kempen and J. S. Brodbelt, *J. Am. Soc. Mass Spectrom.*, 1998, **9**, 1049; W. Z. Shou and R. F. Browner, *Anal. Chem.*, 1999, **71**, 3365.
22 U. Yoshio, *Pure Appl. Chem.*, 1995, **67**, 507.
23 G. Horvai, K. Toth and E. Pungor, *Anal. Chim. Acta*, 1976, **82**, 45.
24 D. Ammann, P. Anker, E. Metzger, U. Oesch and W. Simon, in *Ion Measurements in Physiology and Medicine*, Eds. M. Kessler, J. Hopper and D. K. Harrison, Springer-Verlag, Berlin, Heidelberg, 1985.
25 P. Anker, D. Ammann, P. C. Meier and W. Simon, *Clin. Chem.*, 1984, **30**, 454.
26 M. L. Bishop, J. L. Duben-Engelkirk and E. P. Fody, Eds., in *Clinical Chemistry: Principles, Procedures, Correlations*, 2nd Edn., J. B. Lippincott, Philadelphia, USA, 1992, Ch. 11.

Paper a909906i